J Med Ultrasonics (2006) 33:143–151
DOI 10.1007/s10396-005-0095-2

ORIGINAL ARTICLE

Hideyuki HASEGAWA · Hiroshi KANAI

Measurement of nonlinear property of artery wall using remote cyclic actuation

Received: October 31, 2005 / Accepted: December 26, 2005

Abstract
Purpose. For tissue characterization of the arterial wall, we developed a "phased tracking" method to measure the strain (change in wall thickness) and elasticity of the arterial wall. To improve the accuracy of tissue characterization, we are now attempting to measure other mechanical properties in addition to elasticity.
Methods. In this study, the change in elasticity during the cardiac diastole was measured with ultrasound by generating a change in internal pressure using remote cyclic actuation.
Results. From the measured change in elasticity during cardiac diastole, the nonlinear property in the stress–strain relationship of the artery wall was estimated. In basic experiments using a silicone rubber tube and in vivo experiments in human carotid arteries.
Conclusion. The proposal method enables the noninvasive measurement of the nonlinear mechanical property in addition to the elasticity of the arterial wall.

Keywords remote actuation · internal pressure · wall thickness · nonlinear property in stress–strain relationship · atherosclerosis

Introduction

The steady increase in the number of patients with myocardial infarction or cerebral infarction, both of which are mainly caused by atherosclerosis, is becoming a serious problem. Therefore, it is important to diagnose atherosclerosis in the early stages of the disease. Computed tomography (CT) and magnetic resonance imaging (MRI) are employed for the diagnosis of atherosclerosis. Although they subject patients to physical and mental hardship, they provide information mainly on the shape of the artery, such as the diameter of the lumen. However, the diameter of the lumen is not altered during early-stage atherosclerosis.[1]

Since there are significant differences between the elastic moduli of the normal arterial wall and those of arterial walls affected by atherosclerosis,[2,3] evaluation of the elasticity of the arterial wall is useful for diagnosis of atherosclerosis.[4] In addition to diagnosis of early-stage atherosclerosis, it is also important to diagnose vulnerability to atherosclerotic plaque, because the rupture of plaques may cause acute myocardial infarction and cerebral infarction.[5–7] Evaluation of mechanical properties, such as the elasticity of the atherosclerotic plaque, would be useful for these purposes.

To obtain the circumferential distensibility of the arterial wall in the plane perpendicular to the axial direction of the artery, methods for measurement of the change in artery diameter have been proposed.[8–12] By assuming the artery to be a cylindrical shell, the average elasticity of the entire circumference in the plane has been evaluated.[13–15] However, the regional elasticity of atherosclerotic plaques cannot be obtained by these methods because an artery with atherosclerotic plaque cannot be assumed to be a cylindrical shell with uniform wall thickness.

To characterize tissues in atherosclerotic plaques, a method for measurement of the regional elastic modulus of the arterial wall in patients with or without atherosclerotic plaque is needed. Such a technique for measurement of the spatial distribution of the regional elasticity would be useful for diagnosis of the vulnerability of the atherosclerotic plaque as well as for the diagnosis of early-stage atherosclerosis. For this purpose, we developed the "phased tracking" method, for measurement of the small change in the thickness of the arterial wall (less than 100 μm) due to the heartbeat.[16–26] From basic experiments, the accuracy of measurement of the change in thickness has been found to be less than 1 μm using the phased tracking method.[17,20,21] From the change in thickness measured by using this method, the regional strain and the elasticity of the arterial wall can be noninvasively evaluated.[23,26]

H. Hasegawa (✉) · H. Kanai
Department of Electronic Engineering, Graduate School of Engineering, Tohoku University, 6-6-5 Aoba, Aoba-ku, Sendai 980-8579, Japan
Tel. +81-22-795-7079; Fax +81-22-263-9230
e-mail: hasegawa@us.ecei.tohoku.ac.jp

On the basis of the measured elasticity, it should be possible to discriminate tissues in atherosclerotic plaques, such as fibrous tissue and lipids, because of the large differences in their elasticity.[26] However, it is difficult to discriminate some tissues, such as lipids and blood clots, because of the small differences in their elasticity.[27] Therefore, we are attempting to measure other mechanical properties.

In the literature, it has been reported that the nonlinear property in the stress–strain relationship of the artery wall is different in normal and atherosclerotic artery walls.[28,29] Thus, such a nonlinear property has the potential to improve tissue characterization based on the mechanical properties of the artery wall.

There have been several studies on measurement of the nonlinear elasticity of soft tissue. Catheline et al. investigated the measurement of stress-dependent change in the propagation speed of shear waves generated by ultrasound-induced acoustic radiation force.[30] Erkamp et al. and Nitta and Shiina investigated measurement of the nonlinear relationship between strain and applied stress.[31,32]

In the present study, a method for assessing the nonlinear property in the stress–strain relationship of the artery wall was investigated. For this purpose, external cyclic actuation was applied from the skin surface on the brachial artery.[33,34] The resultant change in internal pressure propagates along the artery, causing changes in the diameter and wall thickness at the carotid artery. By measuring the change in wall thickness of the carotid artery with transcutaneous ultrasound and the change in blood pressure at the radial artery with an applanation tonometer, the change in elasticity during the cardiac diastole and the nonlinear property were obtained noninvasively.

Principles

Measurement of the change in wall thickness using the phased tracking method

For measurement of the small change in wall thickness, the phase shift of an echo, which is caused by the displacement of an object, is estimated from two consecutive echoes.[16] For this purpose, quadrature demodulation is applied to the received ultrasonic waves reflected by the object, and then the in-phase and the quadrature signals are A/D converted. From the demodulated signal, $z(t;\ d + x(t))$, reflected at depth $d + x(t)$ at time t, where d and $x(t)$ are the initial depth set at $t = 0$ and the displacement of the object in the direction of depth, respectively, the phase shift, $\Delta\varphi(t)$, between two consecutive echoes is obtained from the complex cross-correlation function calculated for $M + 1$ samples in the direction of depth as follows:

$$e^{j\Delta\varphi(t)} = \frac{\sum_{m=-M/2}^{M/2} z\left(t+T;\, d+x(t)+mD\right)\cdot z^{*}\left(t;\, d+x(t)+mD\right)}{\left|\sum_{m=-M/2}^{M/2} z\left(t+T;\, d+x(t)+mD\right)\cdot z^{*}\left(t;\, d+x(t)+mD\right)\right|}, \tag{1}$$

where D and T are the spacing of sampled points in the depth direction and the pulse repetition interval, respectively, and * represents the complex conjugate. In measurement of the change in thickness, $M + 1$ in Eq. 1 is set at 5 (= 0.4 μs) in consideration of the pulse length of 0.46 μs.

From the estimated phase shift, $\Delta\hat{\varphi}(t)$, velocity, $v(t)$, of the object is obtained as follows:

$$\hat{v}(t) = -\frac{c_0}{2\omega_0}\frac{\Delta\hat{\varphi}(t)}{T}, \tag{2}$$

where ω_0 and c_0 are the center angular frequency of the ultrasonic pulse and the speed of sound, respectively.

In estimation of the phase shift by Eq. 1, the object position is tracked by integrating the average velocity, $v(t)$, during the pulse repetition interval, T, as follows:

$$\begin{aligned}\hat{x}(t+T) &= \hat{x}(t) + \hat{v}(t)\times T \\ &= \hat{x}(t) - \frac{c_0}{2\omega_0}\Delta\hat{\varphi}(t).\end{aligned} \tag{3}$$

From displacements, $x_A(t)$ and $x_B(t)$, of two points, which are set in the arterial wall along an ultrasonic beam, the small change in thickness, $\Delta h(t)$, between these two points is obtained as follows:

$$\begin{aligned}\Delta\hat{h}(t) &= \hat{x}_A(t) - \hat{x}_B(t) \\ &= \int_0^t \left\{\hat{v}_A(t) - \hat{v}_B(t)\right\} \mathrm{d}t.\end{aligned} \tag{4}$$

The accuracy in measurement of the change in thickness was validated to be 0.2 μm by basic experiments using a rubber plate.[21]

Elastic modulus obtained by measuring change in wall thickness

From the measured change in wall thickness, the circumferential elastic modulus is obtained as follows:[23] under a two-dimensional stress–strain relationship in the plane that is perpendicular to the axis of the artery, the radial incremental strain, $\Delta\varepsilon_r(t)$, which is defined by dividing the change in thickness, $\Delta h(t)$, by the original wall thickness, h_0, is expressed by the radial and the circumferential incremental stresses, $\Delta\sigma_r(t)$ and $\Delta\sigma_\theta(t)$, as follows:

$$\begin{aligned}\Delta\varepsilon_r(t) &= \frac{\Delta h(t)}{h_0} \\ &= \frac{\Delta\sigma_r(t)}{E_r} - \nu\frac{\Delta\sigma_\theta(t)}{E_\theta},\end{aligned} \tag{5}$$

where E_r, E_θ, and ν are the radial and the circumferential elastic moduli and Poisson's ratio, respectively.

From the change in internal pressure, $\Delta p(t)$, the circumferential and the radial incremental stresses, $\Delta\sigma_r(t)$ and $\Delta\sigma_\theta(t)$, are expressed as follows:

$$\Delta\sigma_\theta(t) = \frac{r_0}{h_0}\Delta p(t), \tag{6}$$

$$\Delta\sigma_r(t) = -\frac{1}{2}\Delta p(t), \tag{7}$$

where r_0 is the inner radius at the end diastole.

By substituting Eqs. 6 and 7 into Eq. 5, Eq. 5 is rewritten as follows:

$$\Delta\varepsilon_r(t) = -\frac{1}{2}\frac{\Delta p(t)}{E_r} - \nu\frac{r_0}{h_0}\frac{\Delta p(t)}{E_\theta}. \tag{8}$$

By assuming that the arterial wall is incompressible ($\nu \approx 0.5$), Eq. 8 can be rewritten as follows:

$$E_\theta = \frac{1}{2}\left(\frac{r_0}{h_0} + \frac{E_r}{E_\theta}\right)\frac{\Delta p(t)}{-\Delta\varepsilon_r(t)}. \tag{9}$$

Furthermore, by assuming isotropy ($E_r \approx E_\theta$), the elastic modulus, E_θ^h, obtained from the change in wall thickness is defined as follows:

$$E_\theta^h = \frac{1}{2}\left(\frac{r_0}{h_0} + 1\right)\frac{\Delta p(t)}{-\dfrac{\Delta h(t)}{h_0}}. \tag{10}$$

The accuracy in measurement of E_θ^h was validated to be about 8% by basic experiments using silicone rubber tubes with uniform and non-uniform wall thicknesses.[23,24]

Estimation of the nonlinear parameter

The stress–strain relationship of the arterial wall is nonlinear, and this nonlinearity between the pressure increment, Δp, (incremental stress) and the incremental strain, $\Delta\varepsilon_r$, can be modeled using an exponential function as follows:[15]

$$\Delta p = p_0 \cdot e^{\alpha\cdot\Delta\varepsilon_r}, \tag{11}$$

where p_0 and α are the diastolic blood pressure and a parameter showing the degree of nonlinearity, respectively.

The elastic modulus, E_θ^h, in Eq. 10 can be expressed as follows:

$$E_\theta^h = K\frac{\partial\Delta p}{\partial\Delta\varepsilon_r} = \alpha\cdot K\cdot p_0\cdot e^{\alpha\cdot\Delta\varepsilon_r}, \tag{12}$$

where $K = 0.5(r_0/h_0 + 1)$. Equation 12 is rewritten as follows:

$$\begin{aligned}\ln\left(E_\theta^h\right) &= \ln\left(\alpha\cdot K\cdot p_0\right) + \alpha\cdot\Delta\varepsilon_r \\ &= \alpha\cdot\Delta\varepsilon_r + \ln\left(E_0\right),\end{aligned} \tag{13}$$

where E_0 is the elastic modulus at diastolic blood pressure ($\Delta\varepsilon_r = 0$).

It is found that the nonlinear parameter, α, can be obtained from the slope of the relationship between the incremental strain, $\Delta\varepsilon_r$, and the natural logarithm of the elastic modulus, $\ln(E_\theta^h)$.

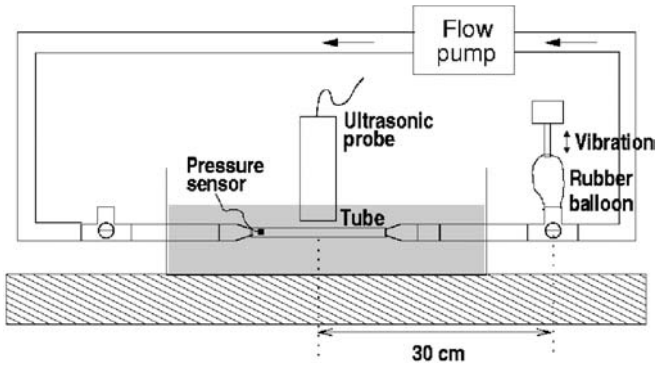

Fig. 1. Basic experimental setup

Basic experiments using a silicone rubber tube

Experimental setup

Basic experiments using a silicone rubber tube (inner radius: 6 mm; outer radius: 8 mm) were conducted to confirm that the relationship between the strain and elastic modulus is measured by application of remote actuation. Figure 1 shows a schematic diagram of the basic experimental setup. In this setup, the pulse pressure was generated by a flow pump, and the cyclic remote actuation at f_{ac} = 10 Hz was applied at a position 30 cm away from the measured position. Resultant changes in internal pressure and wall thickness were measured with a pressure transducer placed inside the tube and with ultrasound, respectively.

Basic experimental results

Figure 2 shows the changes in internal pressure and wall thickness. By referring to the M-mode image shown in Fig. 2a, two points, A and B, were set at the outside and inside of the anterior wall at $t = 0$. Then, velocities, $v_A(t)$ and $v_B(t)$, of these two points were measured by the phased tracking method, as shown in Fig. 2d,e. By integrating the difference between these two velocities, $v_A(t)$ and $v_B(t)$, the change in thickness, $\Delta h(t)$, of the anterior wall was obtained, as shown in Fig. 2f.

To obtain instantaneous amplitudes, $A_{\Delta p}(t = nT; f_{ac})$ and $A_{\Delta h}(t = nT; f_{ac})$ (n = 1, 2, . . . , N; where T is the sampling interval for blood pressure and change in thickness, and N is the number of samples), of changes in blood pressure and wall thickness caused by remote actuation, discrete Fourier transform was applied to the change in wall thickness, $\Delta h(t)$, and blood pressure, $\Delta p(t)$, at each time t with a Hanning window with a length of $\pm 1/f_{ac}$. From the estimated amplitudes, $A_{\Delta p}(t; f_{ac})$ and $A_{\Delta h}(t; f_{ac})$, the elastic modulus at each time was obtained based on Eq. 10. During the period from 0.6 s to 1.0 s after each trigger for the flow pump, which simulates the cardiac diastole, the elastic modulus was plotted as a function of the mean strain during the corresponding time window, as shown in Fig. 3. In Fig. 3, solid curves are shown for ten beats of the flow pump. It was found that the

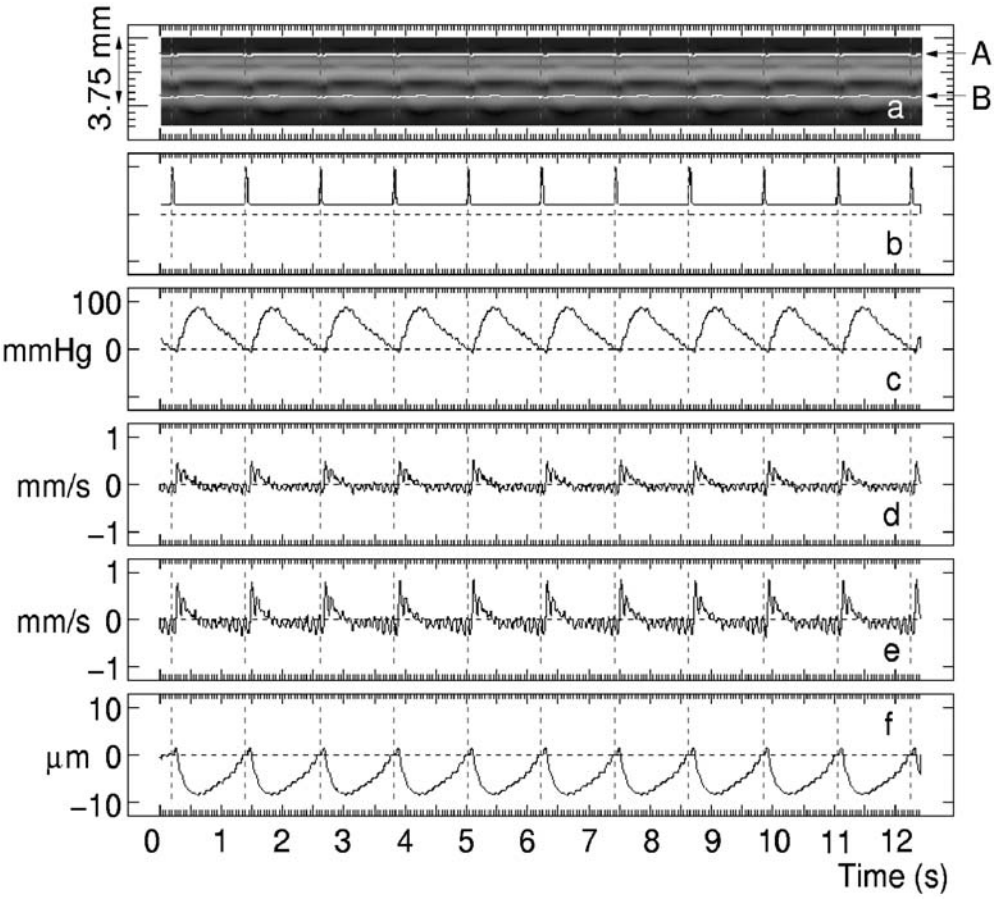

Fig. 2. **a** M-mode image of the silicone rubber tube. (A: external surface, B: luminal surfac). **b** Drive signal of the flow pump. **c** Internal pressure. **d** Velocity, $v_A(t)$, at the outside of the anterior wall. **e** Velocity, $v_B(t)$, at the inside. **f** Change in thickness, $\Delta h(t)$, of the anterior wall

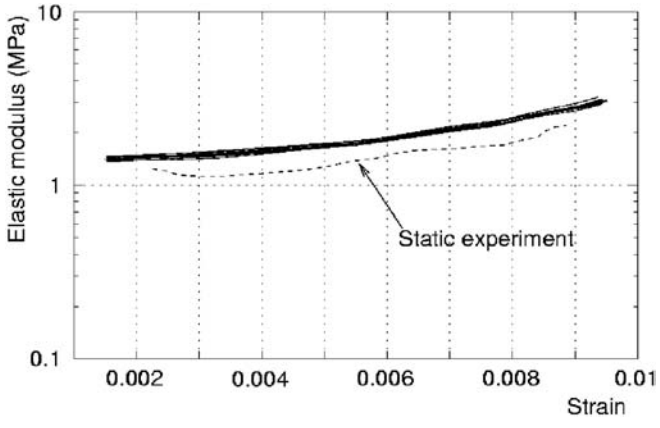

Fig. 3. Relationships between the incremental strain and elastic modulus measured using remote actuation (*solid line*) and the static experiment (*dashed line*)

elastic modulus increased with the mean incremental strain, and the nonlinear parameter, α, was estimated to be 98.6 from the mean curve of the relationship between the strain and elastic modulus.

For comparison with the ultrasonic measurement, the nonlinear parameter, α, was also measured using a quasi-static experiment. In this static experiment, the internal pressure was increased with an air pump by about 15 mmHg/s, and the resultant change in wall thickness was measured with ultrasound. The elastic modulus at each strain level was determined, as shown by the dashed line in Fig. 3, by estimating the slope of the stress–strain relationship using the least-squares method. The nonlinear parameter, α, obtained using this quasi-static experiment was 97.3. Nonlinear parameters, α, obtained using the measurement with remote actuation and the static experiment were found to be in good agreement. In Fig. 3, it was supposed that the elasticity measured using remote actuation was slightly biased relative to that measured using the static experiment due to the difference between the dynamic and the static elastic modul.[34,35]

In vivo experiments at the human carotid artery

Investigation of effective actuation frequency

In in vivo experiments, remote actuation was applied at the skin surface on the brachial artery. The change in internal pressure caused by remote actuation propagates along the artery, and it causes a change in wall thickness at the carotid artery. In this section, an effective actuation frequency for actuating the artery wall was investigated. For in vivo experiments, an actuation system designed to change the actuation frequency heartbeat by heartbeat was constructed.

In this system, a custom-made computer with A/D and D/A converters controlled the actuation frequency and timing. The R-wave of the electrocardiogram was used as a trigger. The actuation was started at the time of the R-wave. At 0.6 s after the R-wave, the system stopped actuation and changed actuation frequency before the next R-wave.

As shown in Fig. 4, an actuator (MS-VE-01N; IMV, Osaka, Japan) was attached to the skin surface above the brachial artery using a cuff and a belt, and it was tightly fixed by pressurizing the cuff. The actuator was heavy (about 15 kg) to reduce undesired vibration of the entire arm.

Figure 5 shows the results measured at a carotid artery of a 30-year-old man with a linear-type probe of 7.5 MHz.

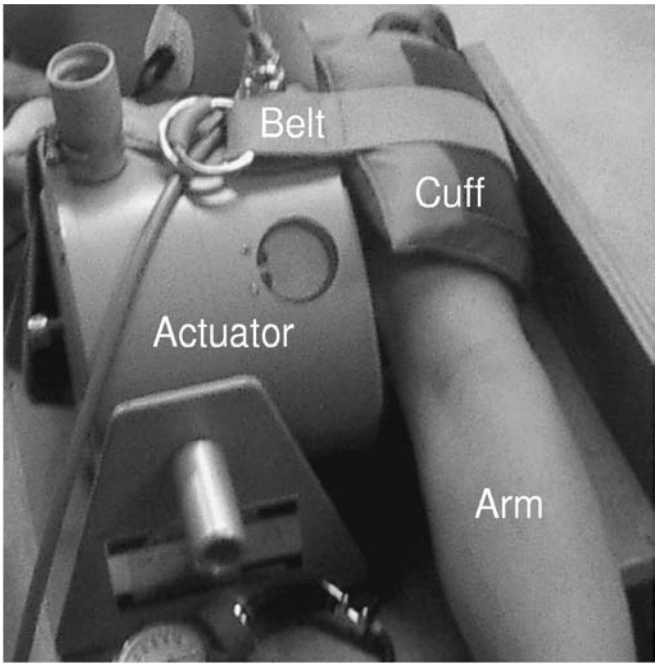

Fig. 4. Actuator used in the in vivo experiments

At a time $t = 0$, a point to be tracked was manually assigned by referring to the M-mode image shown in Fig. 5a. Then, the velocity of the assigned point was obtained by using the phased tracking method, as shown in Fig. 5c. In this measurement, the actuation frequency was cyclically changed from 10 Hz to 20 Hz heartbeat by heartbeat. It was found that the velocity component of the arterial wall caused by remote actuation in cardiac diastole peaks at a frequency of 13 Hz. Therefore, in the following section, the nonlinear parameter, α, was investigated at an actuation frequency of $f_{ac} = 13$ Hz.

In Fig. 6, the velocities of the anterior and posterior walls were measured at an actuation frequency of 13 Hz. The phase difference between velocity components of the anterior and posterior walls caused by remote actuation was about 180°, which shows that the change in diameter was caused by remote actuation. From this result, it was supposed that the change in internal pressure at the carotid artery was successfully generated by remote actuation.

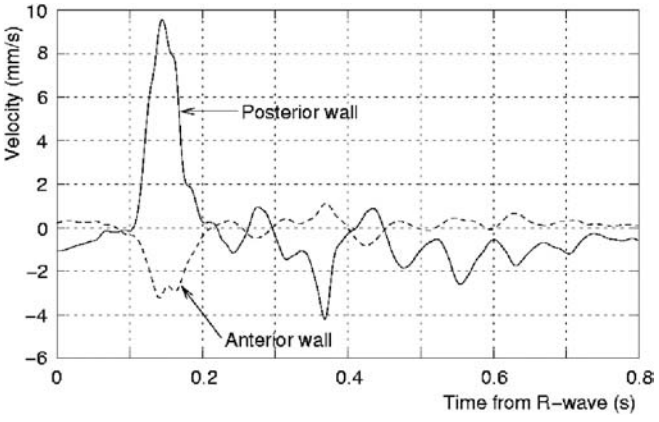

Fig. 6. Velocities of the anterior (*dashed line*) and posterior (*solid line*) walls measured at an actuation frequency of 13 Hz

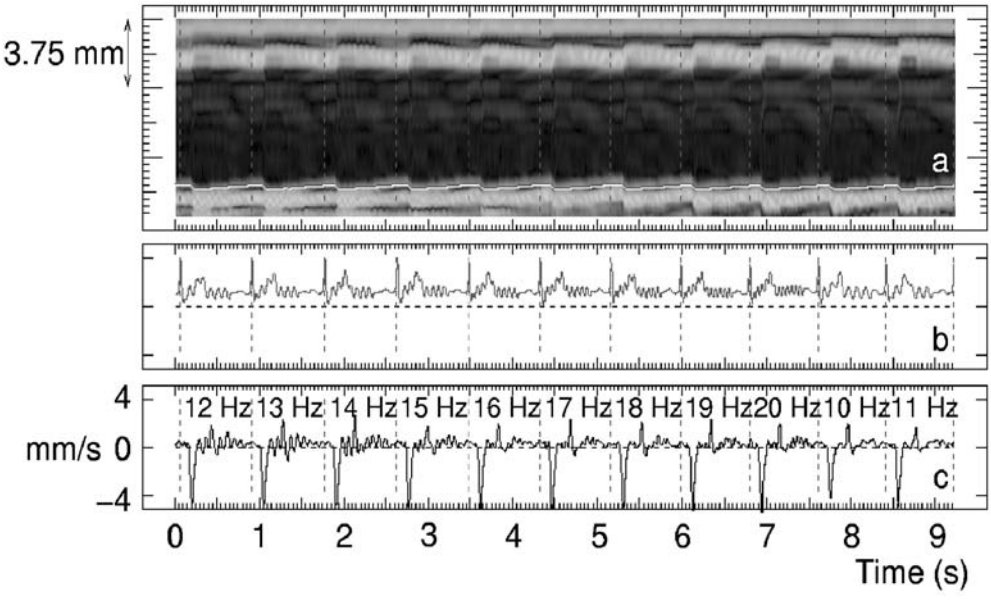

Fig. 5. **a** M-mode image of a carotid artery of a 30-year-old man. **b** Electrocardiogram. **c** Velocity of the posterior wall

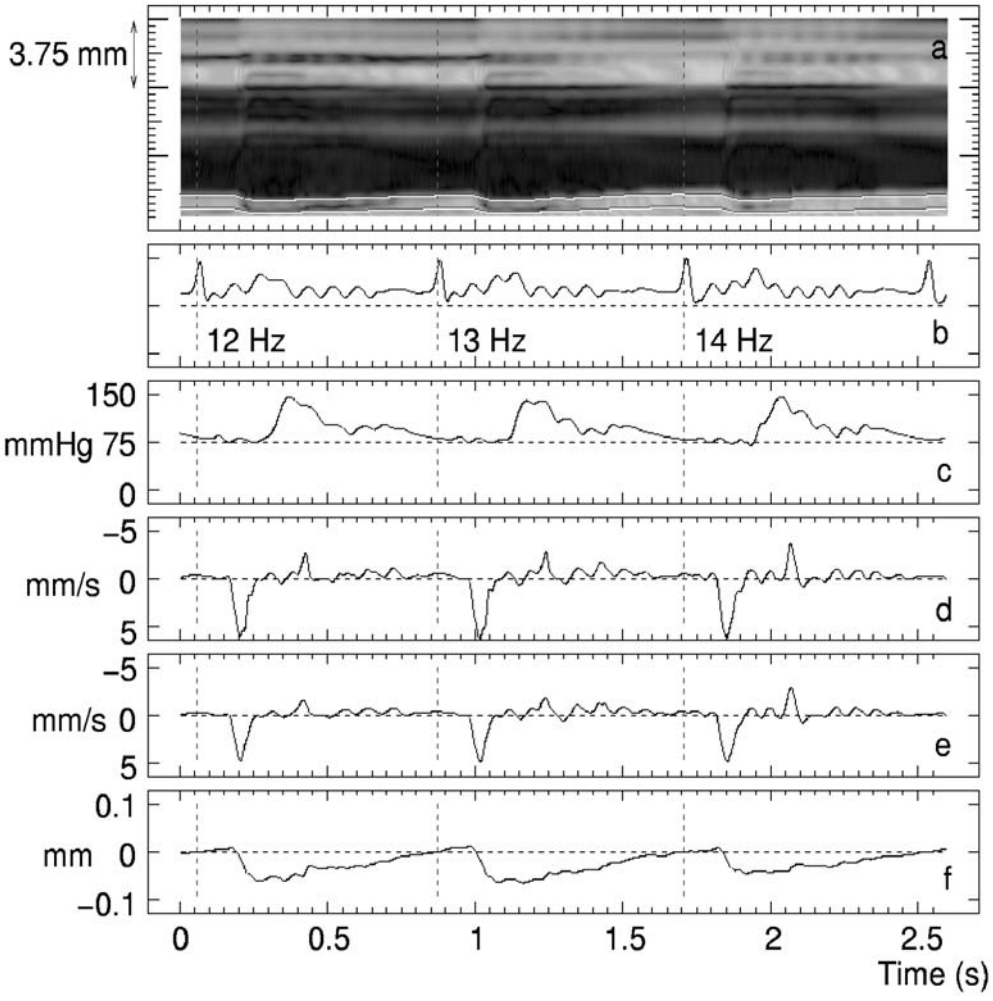

Fig. 7. **a** M-mode image of a carotid artery of a 30-year-old man. **b** Electrocardiogram. **c** Blood pressure measured at the radial artery with an applanation tonometer. **d** Velocity, $v_{in}(t)$, at the inside of the posterior wall. **e** Velocity, $v_{ad}(t)$, at the outside. **f** Change in thickness, $\Delta h(t)$, of the posterior wall

Measurement of the nonlinear parameter

Figure 7a shows the M-mode image of the carotid artery of the same 30-year-old man. Figure 7c shows the blood pressure measured at the radial artery with an applanation tonometer. At the time of the R-wave of the electrocardiogram shown in Fig. 7b, two points were assigned at the intimal and adventitial sides. Then, velocities, $v_{in}(t)$ and $v_{ad}(t)$, of these two points were estimated using the phased tracking method, as shown in Figs. 7d and 7e, respectively. By integrating the difference between these two velocities, the change in thickness, $\Delta h(t)$, of the posterior wall was obtained, as shown in Fig. 7f. For comparison, measurements were also performed at actuation frequencies of f_{ac} = 12 Hz and 14 Hz.

As was the case in the basic experiments, discrete Fourier transform was applied to the change in wall thickness, $\Delta h(t)$, and blood pressure, $\Delta p(t)$, at each time t with a Hanning window with a length of $\pm 1/f_{ac}$ to obtain instantaneous amplitudes, $A_{\Delta p}(t = nT; f_{ac})$ and $A_{\Delta h}(t = nT; f_{ac})$ ($n = 1, 2, \ldots$; where T is the sampling interval for waveforms of blood pressure and change in thickness), of changes in blood pressure and wall thickness caused by remote actuation. From the estimated amplitudes, $A_{\Delta p}(t; f_{ac})$ and $A_{\Delta h}(t; f_{ac})$, the elastic modulus at each time was obtained based on Eq. 10. In Figs. 8a,b, the elastic modulus and mean incremental strain during the Hanning window at each time t were plotted as functions of time t from the R-wave of an electrocardiogram. A similar tendency was found in the results obtained at frequencies of 12, 13, and 14 Hz. The rapid increase in the elastic modulus around t = 0.6 s at an actuation frequency of 13 Hz was supposed to be influenced by the stoppage of actuation for preparing for the next heart cycle. Therefore, the measured elasticity from 0.58 s to 0.6 s after the R-wave was eliminated for the actuation frequency of 13 Hz. Figure 9 shows the relationship between the elastic modulus and mean incremental strain. It was found that the elastic modulus increased with mean incremental strain and that there were similar tendencies in the results obtained at actuation frequencies of 12, 13, and 14 Hz. Learoyd and Taylor reported that the elastic modulus of the human carotid artery changes in the range from 0.5 MPa (80 mmHg) to 1.0 MPa (100 mmHg) in in vitro experiments.[35] The change in elasticity noninvasively measured by the proposed method was in a similar range.

In Fig. 10, elastic moduli measured at the carotid arteries of healthy 30-year-old and 22-year-old men were plotted as a function of mean incremental strain (actuation fre-

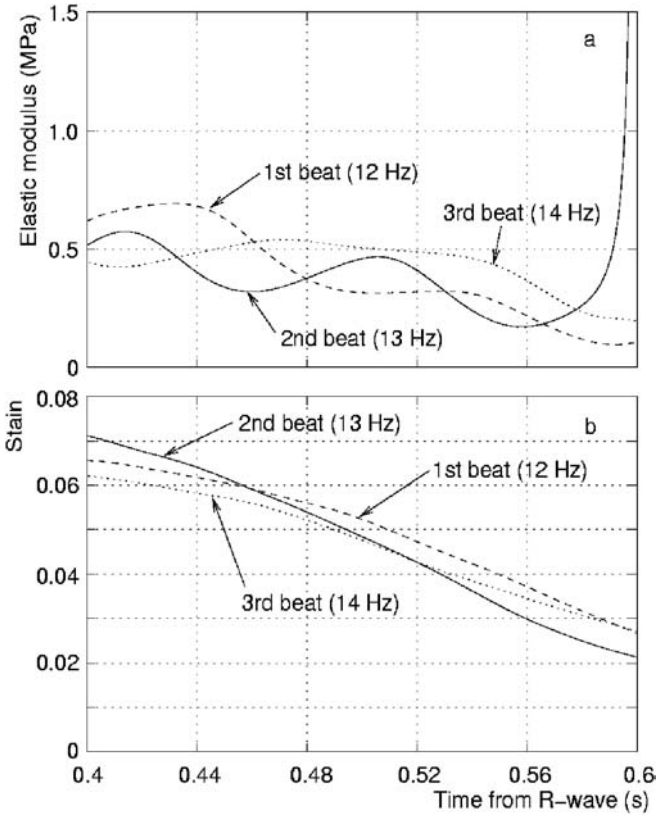

Fig. 8. Elastic modulus (**a**) and incremental strain (**b**) plotted as functions of time

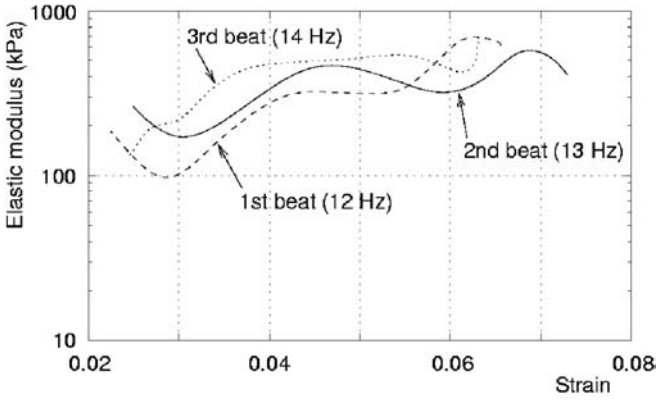

Fig. 9. Relationship between incremental strain and logarithm of the elastic modulus, $\ln(E_\theta^h)$, of a carotid artery of a healthy 30-year-old man at frequencies of 12, 13, and 14 Hz

quency: 13 Hz). The range of mean incremental strain of the 22-year-old man was lower than that of the 30-year-old man because the pulse pressure of the 22-year-old man (≈30 mmHg) due to the heartbeat was smaller than that (50 mmHg) of the 30-year-old man. As shown in Fig. 10, it was found that the elastic modulus of the 22-year-old man also increased with mean incremental strain as well as that of the 30-year-old man. These results show the potential of the proposed method for noninvasive assessment of the

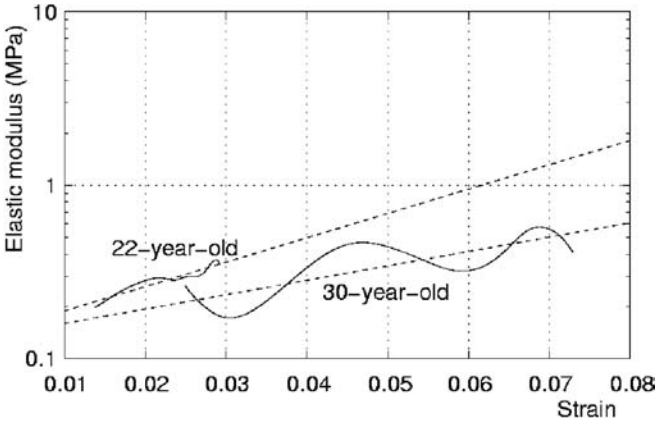

Fig. 10. Relationship between incremental strain and logarithm of the elastic modulus, $\ln(E_\theta^h)$, of the carotid arteries of healthy 30-year-old and 22-year-old men (actuation frequency: 13 Hz)

nonlinear stress–strain relationship of the arterial wall. Finally, nonlinear parameters, α, for the 30-year-old and 22-year-old men were determined to be 19.1 and 32.3, respectively.

Discussion

In this study, an applanation tonometer was used in in vivo experiments for measuring blood pressure waveforms. The change in blood pressure at the carotid artery caused by remote actuation could be estimated by the blood pressure waveform measured at the radial artery because the distance between the brachial artery (actuated point) and the carotid artery is similar to that between the brachial artery and the radial artery (measured with an applanation tonometer). However, the distance between the heart and the carotid artery is very much different from that between the heart and the radial artery, and the change in blood pressure at the carotid artery caused by the heartbeat cannot be estimated by the blood pressure waveform measured with an applanation tonometer. Therefore, in this study, elastic moduli were plotted as a function of the strain measured at the carotid artery.

Sugawara et al. reported that the change in diameter of the carotid artery almost coincided with the blood pressure waveform at the carotid artery.[36] Therefore, there is a possible alternative way in which the change in diameter of the carotid artery is used for the blood pressure waveform. Using the waveform of the change in diameter, which was measured using the phased tracking method and was calibrated by the maximum and minimum blood pressure, the elastic modulus at each time was estimated and plotted as a function of strain, as shown in Fig. 11. In Fig. 11, the elastic modulus became almost constant. One of the reasons for this result might be as follows: in the transcutaneous measurement of the blood pressure waveform, the strain of an employed sensor, which is caused by the blood pressure, must be calibrated by the maximum and minimum blood

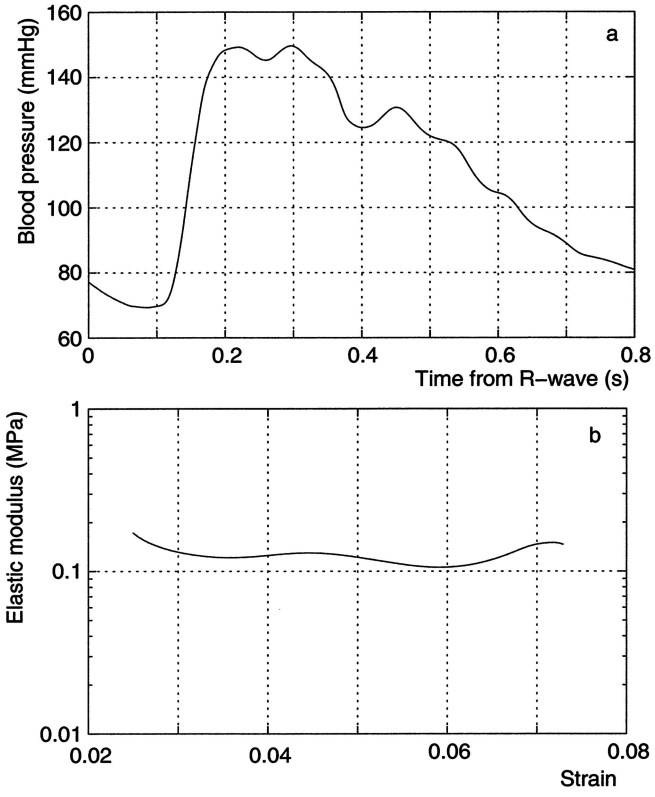

Fig. 11. **a** Blood pressure waveform obtained by calibrating the change in diameter measured by the phased tracking method using maximum and minimum blood pressure measured with a cuff at the upper arm. **b** Relationship between incremental strain and logarithm of elastic modulus, $\ln(E_\theta^h)$, with respect to the same 30-year-old man shown in Fig. 10. The elastic modulus was calculated using the blood pressure waveform obtained from the change in diameter shown in Fig. 11a. The actuation frequency was 13 Hz

pressure. An applanation tonometer calibrates the strain of a transducer tightly attached to the skin surface above the radial artery. In this case, the nonlinearity in the stress–strain relationship of the transducer material is negligible. However, the nonlinearity cannot be neglected when the strain of the artery wall (change in diameter) is calibrated. Slight nonlinearity was found in the stress–strain relationship of the carotid artery wall.[36]

Conclusion

In this paper, a preliminary study was conducted for assessment of the nonlinear property in the stress–strain relationship of the artery wall. A change in internal pressure was caused by remote cyclic actuation applied at the brachial artery to generate a change in the thickness of the arterial wall. From the measured changes in wall thickness and blood pressure, the instantaneous elastic modulus during diastole was obtained. It was found that the elastic modulus decreased in relation to the decrease in the incremental strain during cardiac diastole, and the nonlinear parameter was estimated from the slope of the relationship between the incremental strain and elastic modulus. Such a method for assessment of the nonlinear property in the stress–strain relationship of the artery wall will be useful for the diagnosis of atherosclerosis. In future work, more in vivo data should be investigated to show the clinical feasibility of the proposed method.

Acknowledgment This research was supported by the Research and Development Committee Program of the Japan Society of Ultrasonics in Medicine.

References

1. Glagov S, Weisenberg E, Zarins CK, et al. Compensatory enlargement of human atherosclerotic coronary arteries. New Engl J Med 1987;316:1371–5.
2. Lee RT, Grodzinsky AJ, Frank EH, et al. Structure-dependent dynamic mechanical behavior of fibrous caps from human atherosclerotic plaques. Circulation 1991;83:1764–70.
3. Loree HM, Grodzinsky AJ, Park SY, et al. Static circumferential tangential modulus of human atherosclerotic tissue. J Biomech 1994;27:195–204.
4. Simons PCG, Algra A, Bots ML, et al. Common carotid intima-media thickness and arterial stiffness. Circulation 1999;100:951–7.
5. Falk E, Shah PK, Fuster V. Coronary plaque disruption. Circulation 1995;92:657–71.
6. Davies MJ. Stability and instability: two faces of coronary atherosclerosis. Circulation 1996;94:2013–20.
7. Golledge J, Greenhalgh RM, Davies AH. The symptomatic carotid plaque. Stroke 2000;31:774–81.
8. Hoeks APG, Ruissen CJ, Hick P, et al. Transcutaneous detection of relative changes in artery diameter. Ultrasound Med Biol 1985;11:51–9.
9. Länne T, Stale H, Bengtsson H, et al. Noninvasive measurement of diameter changes in the distal abdominal aorta in man. Ultrasound Med Biol 1992;18:451–7.
10. Hoeks APG, Di X, Brands PJ, et al. Comparison of the performance of the RF cross correlation and Doppler autocorrelation technique to estimate the mean velocity of simulated ultrasound signals. Ultrasound Med Biol 1993;19:727–40.
11. Brands PJ, Hoeks APG, Rutten MC, et al. A noninvasive method to estimate arterial impedance by means of assessment of local diameter change and the local center-line blood flow velocity using ultrasound. Ultrasound Med Biol 1996;22:895–905.
12. Meinders JM, Brands PJ, Willigers JM, et al. Assessment of the spatial homogeneity of artery dimension parameters with high frame rate 2-D B-mode. Ultrasound Med Biol 2001;27:785–94.
13. Bergel DH. The static elastic properties of the arterial wall. J Physiol 1961;156:445–57.
14. Peterson LH, Jensen RE, Parnell J. Mechanical properties of arteries *in vivo*. Circ Res 1960;8:622–39.
15. Hayashi K, Handa H, Nagasawa S, et al. Stiffness and elastic behavior of human intracranial and extracranial arteries. J Biomech 1980;13:175–84.
16. Kanai H, Sato M, Koiwa Y, et al. Transcutaneous measurement and spectrum analysis of heart wall vibrations. IEEE Trans Ultrason Ferroelect Freq Contr 1996;43:791–810.
17. Kanai H, Hasegawa H, Chubachi N, et al. Noninvasive evaluation of local myocardial thickening and its color-coded imaging. IEEE Trans Ultrason Ferroelect Freq Contr 1997;44:752–68.
18. Hasegawa H, Kanai H, Chubachi N, et al. Noninvasive evaluation of Poisson's ratio of arterial wall using ultrasound. Electron Lett 1997;33:340–1.
19. Hasegawa H, Kanai H, Chubachi N, et al. Evaluation of the elastic modulus of the arterial wall by accurate noninvasive measurement of change in its thickness. Jpn J Med Ultrason 1997;24:851–60 [in Japanese].

20. Hasegawa H, Kanai H, Hoshimiya N, et al. Accuracy evaluation in the measurement of a small change in the thickness of arterial walls and the measurement of elasticity of the human carotid artery. Jpn J Appl Phys 1998;37:3101–5.
21. Kanai H, Sugimura K, Koiwa Y, et al. Accuracy evaluation in ultrasonic-based measurement of microscopic change in thickness. Electron Lett 1999;35:949–50.
22. Hasegawa H, Kanai H, Hoshimiya N, et al. Reduction of influence of decrease in signal-to-noise ratio in measurement of change in thickness of arterial wall due to heartbeat. Jpn J Appl Phys 2000;39:3257–61.
23. Hasegawa H, Kanai H, Hoshimiya N, et al. Evaluating the regional elastic modulus of a cylindrical shell with nonuniform wall thickness. J Med Ultrason 2004;31:81–90.
24. Hasegawa H, Kanai H, Hoshimiya N, et al. A method for evaluation of regional elasticity of the arterial wall with non-uniform wall thickness by measurement of its change in thickness during an entire heartbeat. IEEE 2000 Int Ultrason Symp Proc 2000;1829–32.
25. Hasegawa H, Kanai H, Koiwa Y. Modified phased tracking method for measurement of change in thickness of arterial wall. Jpn J Appl Phys 2002;41:3563–71.
26. Kanai H, Hasegawa H, Ichiki M, et al. Elasticity imaging of atheroma with transcutaneous ultrasound: preliminary study. Circulation 2003;107:3018–21.
27. Inagaki J, Hasegawa H, Kanai H, et al. Construction of reference data for tissue characterization of arterial wall based on elasticity images. Jpn J Appl Phys 2005;44:4593–7.
28. Newman DL, Gosling RG, Bowden NLR. Changes in aortic distensibility and area ratio with the development of atherosclerosis. Atherosclerosis 1971;14:231–40.
29. Hudetz AG, Mark G, Kovach AGB, et al. Biomechanical properties of normal and fibrosclerotic human cerebral arteries. Atherosclerosis 1981;39:353–65.
30. Catheline S, Bercoff J, Gennisson JL, et al. Nonlinearity studies in soft tissues with the supersonic shear imaging system. IEEE 2004 Int Ultrason Symp Proc 2004;1510–2.
31. Erkamp RQ, Emelianov SY, Skovoroda AR, et al. Nonlinear elasticity imaging: theory and phantom study. IEEE Trans Ultrason Ferroelect Freq Contr 2004;51:532–9.
32. Nitta N, Shiina T. Estimation of nonlinear elasticity parameter of tissues by ultrasound. Jpn J Appl Phys 2002;41:3572–8.
33. Hasegawa H, Kanai H, Koiwa H, et al. Measurement and change in wall thickness of cylindrical shell due to cyclic remote actuation for assessment of viscoelasticity of arterial wall. Jpn J Appl Phys 2003;42:3255–61.
34. Hasegawa H, Kanai H. Measurement of elastic moduli of the arterial wall at multiple frequencies by remote actuation for assessment of viscoelasticity. Jpn J Appl Phys 2004;43:3197–203.
35. Learoyd BM, Taylor G. Alterations with age in the viscoelastic properties of human arterial walls. Circ Res 1966;18:278–92.
36. Sugawara M, Furuhata H, Kikkawa S, et al. Development of a noninvasive method of measuring blood pressure wave. Jpn J Med Electron Biol Eng 1983;21S:429.